Complex-coupled photonic crystal THz lasers with independent loss and refractive index modulation

Hua Zhang,[1] Giacomo Scalari,[2] Mattias Beck,[2] Jérôme Faist,[2] and Romuald Houdré[1,*]

[1]*Institut de Physique de la Matière Condensée, Ecole Polytechnique Fédérale de Lausanne (EPFL), Station 3, Lausanne, CH-1015, Switzerland*

[2]*Institut für Quantenelektronik, Eidgenössische Techniche Hochshule Zürich (ETHZ), Zürich, CH-8072, Switzerland*

**romuald.houdre@epfl.ch*

Abstract: Compared to near infra-red photonic crystal (PhC) band-edge lasers, achieving vertical emission with quantum cascade (QC) material operating in the THz range needs dedicated engineering because the TM polarized emission of QCLs favors in-plane emitting schemes and the currently used double plasmon waveguide, prevents vertical light extraction. We present an approach with independent refractive index and extraction losses modulation. The extraction losses are obtained with small extracting holes located at appropriate positions. The modal operation of the PhC is shown to critically depend on the external losses introduced. Very high surface emission power for optimum loss extractor design is achieved.

OCIS codes: (050.5298) Photonic crystals; (140.5965) Semiconductor lasers, quantum cascade; (260.3090) Infrared, far; (220.4000) Microstructure fabrication.

References and links

1. R. Colombelli, K. Srinivasan, M. Troccoli, O. Painter, C. F. Gmachl, D. M. Tennant, A. M. Sergent, D. L. Sivco, A. Y. Cho, and F. Capasso, "Quantum cascade surface-emitting photonic crystal laser," Science **302**(5649), 1374–1377 (2003).
2. O. P. Marshall, V. Apostolopoulos, J. R. Freeman, R. Rungsawang, H. E. Beere, and D. A. Ritchie, "Surface-emitting photonic crystal terahertz quantum cascade lasers," Appl. Phys. Lett. **93**(17), 171112 (2008).
3. L. Sirigu, R. Terazzi, M. I. Amanti, M. Giovannini, J. Faist, L. A. Dunbar, and R. Houdré, "Terahertz quantum cascade lasers based on two-dimensional photonic crystal resonators," Opt. Express **16**(8), 5206–5217 (2008).
4. Y. Chassagneux, R. Colombelli, W. Maineult, S. Barbieri, H. E. Beere, D. A. Ritchie, S. P. Khanna, E. H. Linfield, and A. G. Davies, "Electrically pumped photonic-crystal terahertz lasers controlled by boundary conditions," Nature **457**(7226), 174–178 (2009).
5. J. P. Dowling, M. Scalora, M. J. Bloemer, and C. M. Bowden, "The photonic band-edge laser - a new approach to gain enhancement," J. Appl. Phys. **75**(4), 1896–1899 (1994).
6. H. Kogelnik and C. V. Shank, "Coupled-wave theory of distributed feedback lasers," J. Appl. Phys. **43**(5), 2327–2335 (1972).
7. E. Kapon, A. Hardy, and A. Katzir, "The effect of complex coupling-coefficients on distributed feedback lasers," IEEE J. Quantum Electron. **18**(1), 66–71 (1982).
8. S. Nojima, "Optical-gain enhancement in two-dimensional active photonic crystals," J. Appl. Phys. **90**(2), 545–551 (2001).
9. O. Demichel, L. Mahler, T. Losco, C. Mauro, R. Green, A. Tredicucci, J. Xu, F. Beltram, H. E. Beere, D. A. Ritchie, and V. Tamosinuas, "Surface plasmon photonic structures in terahertz quantum cascade lasers," Opt. Express **14**(12), 5335–5345 (2006).
10. J. A. Fan, M. A. Belkin, F. Capasso, S. Khanna, M. Lachab, A. G. Davies, and E. H. Linfield, "Surface emitting terahertz quantum cascade laser with a double-metal waveguide," Opt. Express **14**(24), 11672–11680 (2006).
11. S. Kumar, B. S. Williams, Q. Qin, A. W. M. Lee, Q. Hu, and J. L. Reno, "Surface-emitting distributed feedback terahertz quantum-cascade lasers in metal-metal waveguides," Opt. Express **15**(1), 113–128 (2007).
12. H. Zhang, L. A. Dunbar, G. Scalari, R. Houdré, and J. Faist, "Terahertz photonic crystal quantum cascade lasers," Opt. Express **15**(25), 16818–16827 (2007).
13. J. Faist, F. Capasso, D. L. Sivco, C. Sirtori, A. L. Hutchinson, and A. Y. Cho, "Quantum cascade laser," Science **264**(5158), 553–556 (1994).
14. R. Köhler, A. Tredicucci, F. Beltram, H. E. Beere, E. H. Linfield, A. G. Davies, D. A. Ritchie, R. C. Iotti, and F. Rossi, "Terahertz semiconductor-heterostructure laser," Nature **417**(6885), 156–159 (2002).
15. B. S. Williams, "Terahertz quantum-cascade lasers," Nat. Photonics **1**(9), 517–525 (2007).

#143564 - $15.00 USD Received 9 Mar 2011; revised 13 May 2011; accepted 13 May 2011; published 17 May 2011

16. B. S. Williams, S. Kumar, H. Callebaut, Q. Hu, and J. L. Reno, "Terahertz quantum-cascade laser at λ≈100 μm using metal waveguide for mode confinement," Appl. Phys. Lett. **83**(11), 2124–2126 (2003).
17. H. Zhang, G. Scalari, J. Faist, L. A. Dunbar, and R. Houdré, "Design and fabrication technology for high performance electrical pumped terahertz photonic crystal band edge lasers with complete photonic band gap," J. Appl. Phys. **108**(9), 093104 (2010).
18. H. Zhang, G. Scalari, R. Houdré, and J. Faist, "In-plane and surface emitting high performance THz pillar type photonic crystal lasers with complete photonic bandgaps" in *Proceedings of the IEEE Lasers and Electro-Optics 2009 and European Quantum Electronics Conference (CLEO Europe - EQEC 2009)*, DOI 10.1109/CLEOE-EQEC.2009.5192585.
19. COMSOL-Multiphysics, http://www.comsol.com.
20. M. I. Amanti, M. Fischer, G. Scalari, M. Beck, and J. Faist, "Low-divergence single-mode terahertz quantum cascade laser," Nat. Photonics **3**(10), 586–590 (2009).
21. K. Inoue, M. Sasada, J. Kawamata, K. Sakoda, and J. W. Haus, "A two-dimensional photonic crystal laser," Jpn. J. Appl. Phys. **38**(Part 2, No. 2B), L157–L159 (1999).
22. M. I. Amanti, G. Scalari, R. Terazzi, M. Fischer, M. Beck, J. Faist, A. Rudra, P. Gallo, and E. Kapon, "Bound-to-continuum terahertz quantum cascade laser with a single-quantum-well phonon extraction/injection stage," N. J. Phys. **11**(12), 125022 (2009).

1. Introduction

Surface emission is always a challenging task for semiconductor lasers [1,2], especially with quantum cascade (QC) active material operating in the terahertz (THz) range. Photonic crystal (PhC) structures are good candidates to address this issue. Previously reported surface emitting THz PhC QC lasers were based on deep etched hole arrays or on patterning holes in metal while keeping the active area unetched [3,4]. The full potential of PhC was not exploited as these devices were operating around an incomplete photonic-bandgap (PBG) or experienced only a weak refractive index contrast. In this work we present a complex-coupled THz surface emitting structure with periodic extraction losses on a pillar-type PhC pattern, which allows us to independently tailor the refractive index and the extraction loss. As a consequence, low average current densities and very high surface emitting power (in excess of 30 mW) is obtained through such extractors.

The periodic arrangement of an optical medium achieved in PhC structure leads to Bloch mode eigenstates with remarkable properties. The band-edge modes are of particular interest as they are responsible of slow light properties and a large density-of-states. The low group velocity of these states is associated with a significant gain enhancement, proportional to the product of the group index and the confinement factor of the field energy in the gain medium [5]. In a Distributed Feedback (DFB) laser, the complex coupling between the refractive index and gain is based on 1D modulation [6,7]. Adding up dimensions when going from 1D DFB to 2D PhC structures allows a potentially easier scaling of the output power as well as producing symmetric, low divergence beam. A gain enhancement factor larger than in 1D DFB was also predicted [8].

The first reported THz surface emitting devices were a second order DFB laser [9–11] or weakly modulated 2D structures [3] exhibiting an incomplete bandgap and where the entire area is pumped. Instead, we will focus on an approach based on deeply etched pillars that provide a full TM gap, and excellent performances in terms of drive current and high temperature operation thanks to propagation losses reduction combined with the benefit that only the area with a large field overlap is pumped [12]. However, such devices do not allow surface emission as the slow light mode lies outside of the light cone [12]. We show here structures that combine slow light enhancement with vertical emission. Moreover the slow light regime is achieved over large k-vector ranges, which is a necessary condition to achieve small device size over a small number of unit cells.

Compared to near infra-red PhC band-edge lasers, achieving vertical emission with quantum cascade (QC) [13] material operating in the THz range [14,15] needs dedicated engineering because, even if the operating Bloch states lies within the light cone, the TM polarized emission of QCLs favors in-plane emitting schemes and secondly because the currently used [16] double plasmon waveguide, which provides nearly unitary mode confinement, prevents vertical light extraction [12] unless the top metal layer is appropriately

#143564 - $15.00 USD Received 9 Mar 2011; revised 13 May 2011; accepted 13 May 2011; published 17 May 2011

turned semi-transparent. In this work we make use of this apparent drawback to design a vertically emitting structure with independent index and extraction losses modulation.

For TM polarized light, the pillar-type PhC laser is the most suited structure as it exhibits complete in-plane PBGs. After BCB planarization [17], a top continuous metallic layer can be deposited and provides several functionalities: i) It defines the top plasmon layer. ii) It is also used as an electrical contact, which does not suffer from potential electrical leakage [3,4] as the pillars define a non-connected surface. iii) Finally it allows the introduction of an independent extraction loss modulation by opening small holes into the top metal layer at proper selected positions (relative to the pillar positions). These holes introduce periodic losses to the existing system while barely disturbing the overall dispersion.

2. Design

Plane Wave Expansion was used to model the planar pillar type PhC as a 2D system in order to calculate the in-plane band structure (Fig. 1(a)). The real parts of the effective refractive indices are $n_{eff,QCL}$ = 3.565 and $n_{eff,BCB}$ = 1.78 for the double plasmon waveguide with QCL and BCB core, respectively and the filling factor value is 40%. Several complete PBGs can be observed. Around the first bandgap (PBG1), the high symmetry K band-edge and M saddle states with large k-vectors allow intrinsic in-plane emission [12]. Around the second bandgap (PBG2), the Γ band-edge states with wavevector k = 0 lie above the light cone, this allows intrinsic emission in the direction normal to the sample surface [18], as shown in the sketch

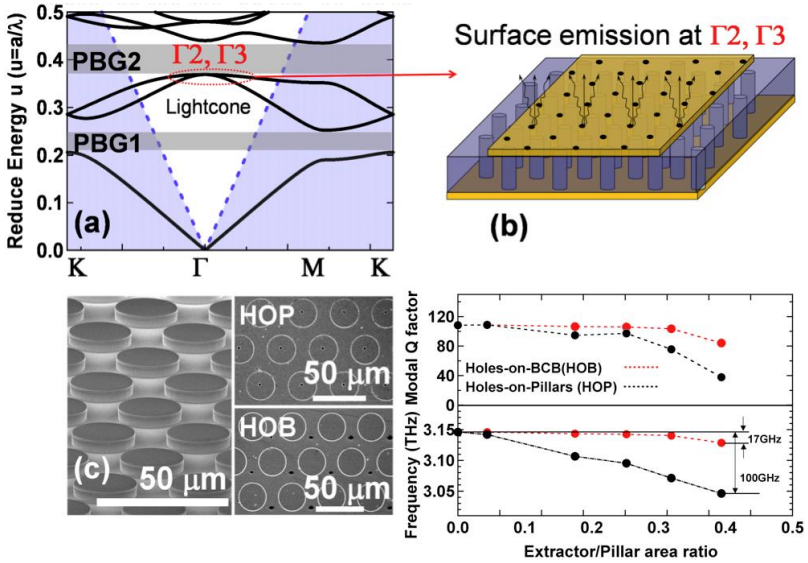

Fig. 1. (a), Photonic crystal dispersion curves calculated by 2D Plane wave expansion, several complete bandgaps are observed (semi-transparent gray shadows, e.g. PBG1 and PBG2). Blue dashed lines indicate the light light. Red dashed circle locates the two slow light band-edge states of interest (Γ2, Γ3). The pillar filling factor (ff) is 40%. (b), Sketch of the surface emitting lasing scheme at the band-edges (Γ2, Γ3). The pillar height is about 15 μm and the lattice constant range is between 32 and 40 μm. (c), Left: Side view SEM image of PhC pillar after dry etching. Top right: Top view SEM image of holes-on-pillars (HOP) device. Bottom right: Top view SEM image of holes-on-BCB (HOB) device. (d), Top panel, extraction modal Q on the Γ3 state as a function of the extractor size. Bottom panel, eigenfrequency on the Γ3 state as a function of the extractor size. The holes-on-pillars (HOP) scheme always has a larger impact on the band structure than the holes-on-BCB (HOB) scheme.

plot of Fig. 1(b). However, because of their parity, these states have a vanishing coupling constant with free space propagating modes that prohibits vertical emission. The extracting small-hole pattern on the top plasmon layer has to be arranged in a fashion that does not match the point group symmetries of the PhC states to achieve a finite coupling in the vertical

#143564 - $15.00 USD Received 9 Mar 2011; revised 13 May 2011; accepted 13 May 2011; published 17 May 2011

direction. An extractor hole pattern centred on a single lobe of the eigenmode is a possible solution, as it breaks one of the mirror symmetry of the mode profile. Note that the same principle of operation for hole extractor holds for the elliptical pillars discussed further. Two different extractor patterns are investigated, with either holes-on-pillars or holes-on-BCB based on a triangular lattice, as shown in the SEM images in Fig. 1(c). 3D simulation [19,20] was performed for the two extraction schemes, to model the impact on eigenfrequencies and the modulation on the eigenstate losses (the metal is assumed as perfect, and the). Figure 1(d) shows the calculated corresponding modulations on the frequency and modal loss of Γ3 band-edge state at different hole sizes. The general rule is that the holes-on-pillars configuration impacts more dramatically both on the frequency and losses than the holes-on-BCB case: The band-edge state frequency for holes-on-BCB configuration shows a negligible shift to the lower frequency; while for holes-on-pillars configuration, the frequency is shifted by values as large as 100 GHz towards lower frequency for 40% of the extractor/pillar surface area ratio. The holes-on-pillars configuration generates a strong index perturbation where the field is maximum. This strongly affects the eigenstate and eigenfrequency of the mode itself. On the other hand in the holes-on-BCB configuration the holes are located where the optical field is weak, the index contrast is less and its perturbation is weaker. Moreover the holes are located where the E-field is parallel to the surface and is more suitable to couple to propagating wave in the vertical direction.

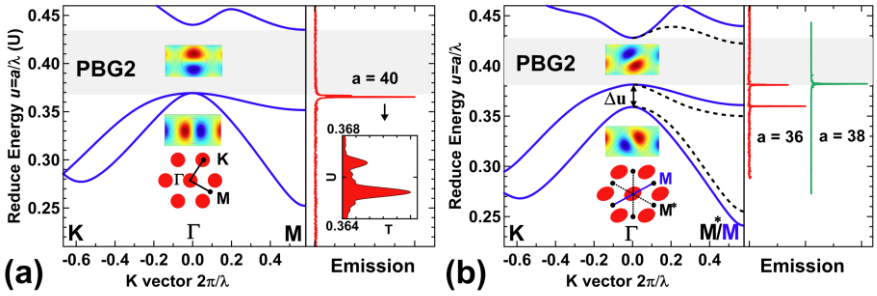

Fig. 2. Elliptical pillar photonic crystal degeneracy lifting. (a) Left, PhC dispersion of circular pillar around PBG2 calculated along k-vector direction of K-Γ-M. E_z field maps of each band-edges (Γ2 and Γ3) are shown as inserts. A schematic drawing of the lattice is inserted with circular pillar configuration. Right, lasing spectra of such circular pillar-PhC laser at a = 40 μm, the zoom region show the multimode behavior at the quasi-degenerated band-edge. (b) Left, PhC dispersion of elliptical pillars calculated along k-vector direction of K-Γ-M. Elliptical pillars are designed with x/y ratio of 0.8, and rotated with 30° angle respective to the horizontal direction. A schematic drawing of the lattice is inserted with elliptical pillar configuration. The degeneracy of the Γ2 and Γ3 band-edge states is lifted. The splitting is about Δu = 0.0224 in reduced energy, which corresponds to a broad frequency bandwidth of 168 GHz at lattice constant a = 40 μm. Right, lasing spectra of such elliptical pillar PhC lasers at a = 36 μm and a = 38 μm. For a = 36 μm, two sharp peaks were observed whose splitting energy is in good agreement with the calculated value Δu = 0.0224 between Γ2 and Γ 3 states. The multimode behavior is due to the gain bandwidth wide enough to overlap with both states. For a = 38 μm, single mode was observed as the gain bandwidth overlaps with only one of the two states (Γ3). The elliptical pillar structure has 6-fold degenerated M points, they split in two groups: a 2-fold of M points, and 4-fold of M* points.

As it can be seen in the magnified dispersion curve of circular pillars in the left panel of Fig. 2(a), the Γ point around PBG2 of the circular pillar structure is doubly degenerated. As these two bands exhibit different slow light enhancement factors [21], this would not be an issue in an ideal system and single mode operation would be achieved on the band with slowest group velocity. However, such configuration is a recipe for poor modal control, especially in a system like QC active material, where an inhomogeneously broadened gain is experienced and the mode degeneracy can be lifted, in an uncontrolled manner, by any residual fabrication disorder or anisotropy. The extractor itself whose function is to generate

#143564 - $15.00 USD Received 9 Mar 2011; revised 13 May 2011; accepted 13 May 2011; published 17 May 2011

out-coupling losses in the vertical direction for the lasing mode will have the counterproductive effect to favour lasing of the not extracted orthogonal mode. This can be solved either with a complex engineering of the extractor with additional losses to prevent lasing on the undesired states. Such approach presents the drawback of an increased lasing threshold. Alternatively, a proper PhC engineering can be used to lift the degeneracy with a sufficiently large frequency splitting. This latter case was used in this work. Figure 2(b) left panel shows the dispersion diagram of an elliptical pillar PhC, with x/y ratio of 0.8, and 30° rotation respective to the horizontal direction. The Γ2 and Γ3 band-edge states degeneracy is then lifted by about Δu = 0.0224 in reduced energy, which corresponds to a broad frequency bandwidth of 168 GHz for lattice constant of a = 40 μm.

3. Device fabrication and characterization

Both circular and elliptical pillars were designed with several different photonic-lattice constants in order to ensure the overlap between the gain bandwidth and the band-edge states at the Γ-point. All the fabricated samples are from the same QC active layer whose wavelength is centred around 3.3 THz, with a gain bandwidth of 0.8 THz [22]. The fabrication and characterization techniques are similar to that described in Refs. [12], [17] and [20]. All the lasers were fabricated with two extraction schemes. The hole extractor is 5 μm wide in diameter, which is assumed to have no effect on the current injection. Note that rather selecting an optimized active material with narrow gain bandwidth for single mode operation, the active material structure was deliberately selected with a very broad gain bandwidth in order to ensure a proof of principle demonstration as well as a PhC singular point spectroscopy around the PBG2. As predicted, the spectra (Fig. 2(a)) of circular pillar PhC laser shows lasing at Γ band-edge frequencies but with undesired multimode behaviour (Figs. 2(a) and 3(b)). On the contrary, elliptical pillar PhC lasers (Fig. 2(b)) show a much more efficient mode control. For smaller lattice constant a = 36 μm, the gain bandwidth is broad enough to excite both the split Γ band-edge states. The measured mode splitting energy between Γ2 and Γ3 states corresponds well to the calculated Δu = 0.0224. For larger lattice constant a = 38 μm, where the gain shifts to higher energy and overlaps with the Γ3 state only, a single mode lasing is observed. For both the circular and elliptical pillar lasers very high surface emission power from the holes-on-BCB extraction scheme was achieved. Figure 3 shows the LIV characterization for circular pillar laser of a = 40 μm. All power measurements have been performed with a terahertz absolute power meter (Thomas Keating Ltd.), which has

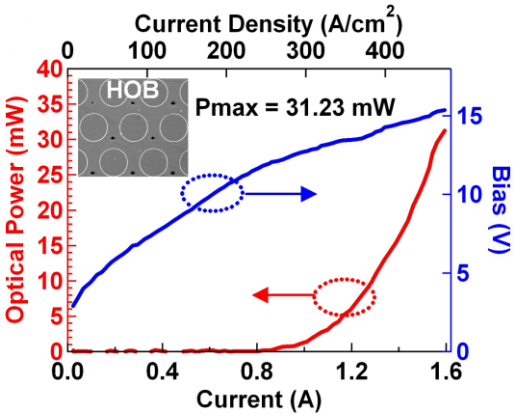

Fig. 3. Light–current–voltage (LIV) a circular pillar type photonic-crystal laser with lattice constant a = 40 μm, with extractor scheme of Holes-on-BCB. The maximum power collected from the top of the device exceeds 31 mW.

a broad surface (6x4 cm^2), placed directly in front of the cryostat window at a distance of 2.5 cm from the laser. This gives a prism of angular aperture 100 deg x 76 deg. The maximum

#143564 - $15.00 USD Received 9 Mar 2011; revised 13 May 2011; accepted 13 May 2011; published 17 May 2011

power collected from the top of the device via the extractors is 31 mW with a differential efficiency value of 67 mW/A, which represents a significant improvement by a factor 4 compared to a double plasmon Fabry-Perot fabricated with the same active material (3 mW and 15 mW/A respectively obtained on a 0.15 mm^2 device).

Finally, in this section, we discuss experimental results on a = 32 µm elliptical pillar structure to investigate the extraction loss modulation scheme. The LIV curves in Fig. 4(a) and Fig. 4(b) show similar threshold currents and maximum operation temperatures. The difference of maximum emitted power between Fig. 3 and 4 can originate from the different lattice constant in both structures, leading to a gain material not operating at the same wavelength. The laser spectra shown in Fig. 4(c) and Fig. 4(d) are measured at different injection currents to investigate the impact of losses on the mode selection. When the injection current is low (≤ 590 mA in both cases), both lasers show mode control as expected from the elliptical pillar dispersion (refer to the elliptical dispersion in Fig. 2(b)). The spectral line positions correspond to the Γ2 mode and the M3* mode (with the elliptical pillar structure the 6-fold degenerated M points, split in two group of a 2-fold (4-fold) M (M*) points, see Fig. 2(b)). However for larger injection currents (> 590 mA), the two structures show different behaviors, the holes-on-pillars scheme turns to multimode rapidly when the injection current is increased. As previously discussed, the holes-on-pillars scheme introduces more losses to the lasing modes, and eventually increases the losses to a comparable level to the losses of the modes induced by any defect cavity or FP-like modes. As a consequence the PhC mode

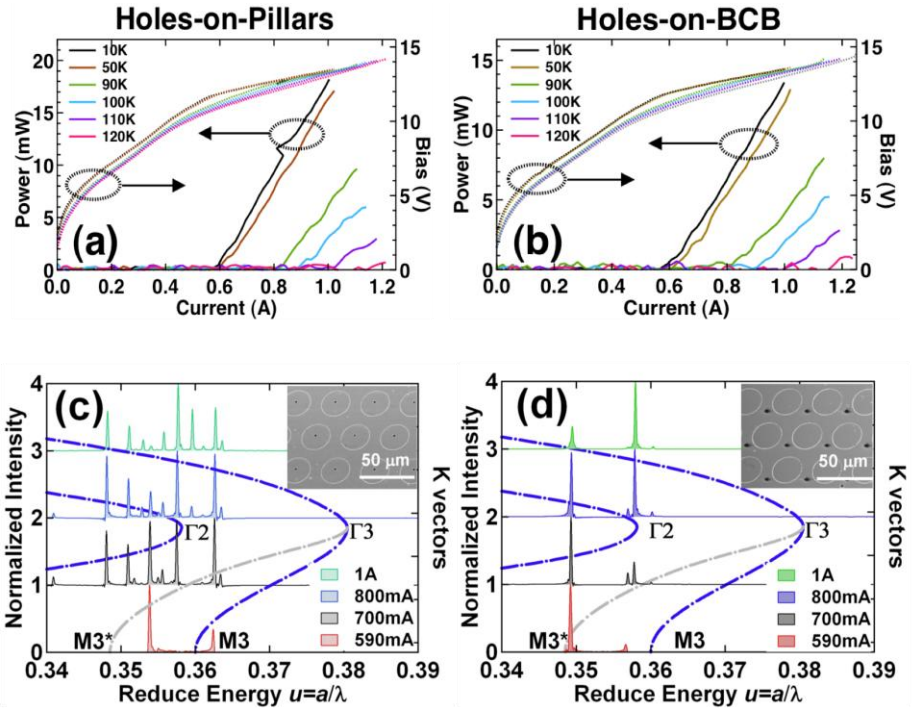

Fig. 4. Light–current–voltage (LIV) and spectral characterizations of elliptical pillar type photonic crystal quantum cascade lasers. (a) and (b), Light–current–voltage (LIV) characteristics as a function of temperature for the two type of extractors. The maximum power collected from the top of the devices are 18.2 mW and 13.4 mW, for holes on pillars and holes on BCB extraction schemes, respectively. The maximum operating temperature for both devices is 120 K, which is the same as the standard FP ridge lasers (embedded with BCB) fabricated on the same batch with the same material. (c) and (d), Dispersion curves and lasing spectra of elliptical pillar-type photonic-crystal lasers at lattice constant a = 32 µm, with holes on pillars and holes on BCB configurations, as shown insert SEM images for (c) and (d), respectively. The intense line at u = 0.35 correspond to lasing at a M3* point.

#143564 - $15.00 USD Received 9 Mar 2011; revised 13 May 2011; accepted 13 May 2011; published 17 May 2011

control is lost and the laser becomes extremely multimode. On the contrary, the PhC lasers with holes-on-BCB extraction scheme display mode control across the entire dynamic range. Preliminary far-fields were performed. Angular narrowing, more pronounced in one direction for the elliptical patterns, could be observed, however some complex structures were observed and further analysis and spectrally resolved data are necessary. It is also well known that achievement of good far-field characteristics relies strongly on a fine optimization of the overall pad shape and boundary conditions, which was not done in the present samples that were mainly designed for a proof of feasibility purpose.

4. Conclusion

We have presented an approach with independent refractive index and extraction losses modulation for surface emitting PhC lasers at THz frequency. The extraction losses is obtained with small extracting holes located at appropriate positions. The modal operation of the PhC was shown to critically depend on the external losses introduced. Very high surface emission power for the optimum loss extractor configuration was achieved. Such approach can be used as a general tool for the development of both electrical and optical pumped devices at any frequencies based on index modulation devices.

Acknowledgments

We thank Maria I. Amanti for the assistant on 3D modelling and Oscar Marchat for his help on device characterization. This work was supported by the Swiss National Science Foundation and the National Center of Competence in Research, Quantum Photonics.

#143564 - $15.00 USD Received 9 Mar 2011; revised 13 May 2011; accepted 13 May 2011; published 17 May 2011